Complex resistivity measurements on plugs from Corvina oil field, Campos basin, Brazil

Leonardo Pereira Marinho (1) and Carlos Alberto Dias (1).
(1) UENF/LENEP, e-mails: leonardomarinho@lenep.uenf.br and diaslenep@gmail.com, respectively.

Abstract

Petrophysical parameters have been measured for 12 plugs from two wells of Corvina oil field, Campos basin, Brazil. Their spectral complex resistivity have been measured in the frequency interval 10^{-3}Hz – 10^{5}Hz, as phase and amplitude. Two models have been used for fitting the experimental data, the Dias model and a new composed Dias/Cole-Cole model. The reasons for introducing this second model was the discrepancies for an intermediate frequency interval when the Dias model was used, presumably due to samples imperfections. In this way, the data fitting problems were solved. The results provide by the two models were used to estimate the values of permeability, successfully in both cases. This analyses also determined the frequency interval to be observed when complex resistivity measurements are taken looking for permeability determination.

Introduction

The electrical characterization of the materials is done through two parameters, the conductivity and the dielectric constant. The first related to the effect due to the "free charge" carries, which are drifted in phase with the applied electric field, and the second one related to the effect due to the "bound" and "semi-free" charges, both carries generating current out phase with the applied electric field.

The presence of interface electrical polarization has been identified as the responsible for the IP phenomenon in rocks, as *electrode polarization* (for disseminated or fracture deposited metallic particles in the porous rock) and *membrane polarization* (for clay minerals disseminated particles in the pores of the rocks).

The two kinds of polarizations can occur in the hydrocarbon reservoir environments, with membrane polarization being the most frequent.

The electrical characterization of a polarizable medium has been reduced by Dias (1968, 1972, 2000) to the determination of the medium constitutive function denominated the *total current conductivity* (or its inverse, the complex resistivity).

A large number of models has been suggested to describe the IP phenomenon as shown and analyzed by Dias (2000). Such analysis concluded that only two models presented the required capacity to fit the experimental data available, the Dias and the double Cole-Cole models, both capable of generating up to two maxima in the phase.

Barreto and Dias (2014) have shown that the first maximum of phase, happening at the lower frequencies, is related to a cation diffusion process through an electrical double layer structure near the interface clay-electrolyte, and the second maximum of phase, at the higher frequencies, is related to a capacitive effect across the double layer. The last authors have shown that the cation diffusion relaxation time can be determined from the first maximum of phase, from which is possible to determine the sample hydraulic permeability.

The objective in this paper is to determine a good theoretical fitting for the IP experimental data obtained with the plugs from the Corvina oil field, Campos basin, and to consolidated the relationship of cation diffusion relaxation time with the rock hydraulic permeability.

Sample petrophysical characteristics and measurements

The rock plugs from the Corvina wells correspond to clayey sandstones with cross section diameter 1.5" (well A) and 1" (well B), and depths between 2,696 m and 2,717 m for A and between 2,712 m and 2,716 m for (B). Samples from a short depth interval of well A were submitted to X-ray analysis (XRD and XRF) for mineral composition determination. The same has not been possible to do with the encapsulated well B samples. The lateral protection with plastics material may have prevented a complete saturation of these plugs before electrical measurements be taken.

Table 1 shows the porosity and permeability values measured in the plugs from the Corvina A and B wells. ***Table 1 -*** *Petrophysical parameters measured in the plugs from Corvina wells.*

Well	Sample ID	Figure ID	Depth (m)	Φ (%)	k (mD)
A	P0818H	A1	2,696.20	21.75	23.08
	P0821H	A2	2,696.80	28.63	82.92
	P0836H	A3	2,700.05	26.80	30.39
	P0897H	A4	2,717.10	28.10	44.94
B	P3806H	A5	2,712.50	19.90	30.65
	P3807V	A6	2,712.80	23.10	6.57
	P3808H	A7	2,713.10	19.70	4.41
	P3810V	A8	2,713,70	16.20	10.37
	P3812V	A9	2,714.30	19.40	2.83
	P3813H	A10	2,714.60	19.00	7.84
	P3817V	A11	2,716.00	17.00	4.92
	P3817H	A12	2,716.00	19.90	5.47

The electrical measurements followed the preparation procedures elaborated by Worthington *et al.* (1990a; 1990b), using for the plugs saturation a NaCl solution 10^{-2} M. After saturation, the samples were placed in a core-holder and an impedance analyzer was used for the measurements.

The experimental data modeling was done in two steps: using the original Dias model, playing with the equations (1) and (2), followed by a second step refining process using a Dias and Cole-Cole composed model given as equation (3). The fitted curves and its respective parameters for cited models are given in the Appendices A and B.

The criterion for fitting the experimental data was the following: (a) to describe the first phase maximum the best possible, because it is critical for estimating the permeability value; (b) the first fitting to be done is using the Dias model, because it will determine the frequency value at which the Cole-Cole maximum should be set, as well as its magnitude and flatness, and avoid multiple solutions.

Modeling the spectral electrical data of samples from wells A and B

Basically the Dias model has been used to describe the experimental data. The samples from Corvina oil field presented many imperfections, such as: geometrical irregularities, the presence of large and micro fractures, and even (for samples from well B) incomplete electrolyte saturation of the plugs. Primarily due to these imperfections, the discrepancies between the data measurements and the Dias model curves required to use sometimes, as a supplementary model, Cole-Cole type curves in the intermediate frequency interval.

Dias model used in the modeling

The original function of this model, as a function of frequency, $\omega = 2\pi f$, where ω is in rad/s and f in Hz, possesses 5 primitive constant parameters $(\rho_0, \mathrm{m}, \tau, \eta, \delta)$ and is given by Dias (2000):

$$\frac{\rho^* - \rho_\infty}{\rho_0} = \frac{m}{1 + i\omega\tau'(1 + 1/\mu)} \qquad (1)$$

where
$i^2 = -1$, $\tau' = [(1-\delta)/(1-\mathrm{m})\delta]\tau$, $\mu = i\omega\tau[1 + \eta(i\omega)^{-1/2}]$
and $\rho_\infty = (1-m)\rho_0$. The parameters ρ_0 and ρ_∞ are the values of ρ^* at the frequencies 0 and ∞, respectively. The definition of the other parameters is as follows: m = chargeability (dimensionless); τ = Helmhotz electrical double layer relaxation time (s); η = electrochemical parameter ($s^{-1/2}$); δ = portion of the medium "unity cell" extension affected by the solid-liquid interface polarization (dimensionless).

When the function (1) is decomposed in partial fractions an "approximated model" results, given by Barreto and Dias (2014):

$$\frac{\rho^* - \rho_\infty}{\rho_0} \simeq \frac{m_w}{1 + (i\omega\tau_w)^{1/2}} + \frac{m_D}{1 + [(i\omega\tau_D)^{1/2} - \nu]^2}\ , \qquad (2)$$
$$+ \text{negligible (terms of 2nd order)}$$

where:

- m_w and m_D: are the partial chargeability, respectively associated to the lower and higher frequencies, with $m_w = m(1-\delta)/(1-\mathrm{m}\,\delta)$, $m_D = m - m_w$;
- f_a: is the factor that measures the effect from the ohmic conduction on the ionic diffusion relaxation time (τ_w), which is given by $\tau_w = (f_a\eta)^{-2}$ and $f_a = \delta(1-\mathrm{m})/(1-m\delta)$;
- τ_w and τ_D: are the relaxation times, respectively at the lower frequencies (related to the ionic diffusion inside the double layer) and at the higher frequencies (related to the capacitive-resistive effect across the double layer), with τ_w (given as before) and $\tau_D = (m_w/m)\tau$;
- ν: second order correction entering term, given by $\nu = -0{,}5(m_w/m)^{3/2}\eta\tau^{1/2}$.

Dias and Cole-Cole composed model

Analyzing the experimental data of amplitude and phase for the samples from Corvina field, it was verified a strong discrepancy of this data compared to the Dias model generated curve in the frequency intermediate range between the two maxima of phase. An intermediate high plateau or, sometimes, an intermediate third maximum show up between the lower frequency maximum and the higher frequency maximum. The modeling data fitting for such cases has led to add a typical Cole-Cole circuit in series with the original Dias model, as shown in Figure 1 circuit.

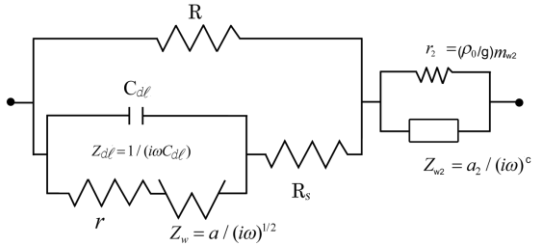

***Figure 1** – Dias and Cole-Cole composed model, where g in the second circuit is the geometric factor equal to S/d, S being the cross section area and d the plug length, and m_{W2} is the contribution to chargeability by the second circuit.*

The expression for the new complex resistivity becomes:

$$\frac{\rho^* - \rho_\infty}{\rho_0} = \frac{m_{w1} + m_D}{1 + i\omega\tau'(1 + 1/\mu)} + \frac{m_{w2}}{1 + (i\omega\tau_{w2})^c}\ , \quad 0 < c \le 1. \qquad (3)$$

Three new parameters (τ_{w2}, m_{w2}, c) are introduced by (3). The first (τ_{w2}) is the relaxation time of a new diffusion-induction "perturbed" process, and the second

(m_{w2}) a corresponding partial chargeability, observed in the intermediate range of frequencies. The third parameter (c) will make the Cole-Cole maximum of phase sharper or flatter. In order to keep coherence with the definition of chargeability given by the expression $m = (\rho_0 - \rho_\infty)/\rho_0$, then m can't be $m = m_{w1} + m_D$ anymore, but $m = m_{w1} + m_D + m_{w2}$.

Results

The Corvina samples phase measurements presented a significant instability at the low frequencies at the very initial interval, particularly for the samples of Figures (A1, A2, A3, A6 and A11). This problem required a data smoothing processing before modeling. This procedure has improved the fitting quality of the critical phase first maximum obtained using both models. The two models have shown also a good performance in describing the phase last maximum for the samples in the figures (A4 - A7) and (A9 - A12). Interesting enough is that three maxima in the phase are exhibited by the samples of two vertical plugs (Figures A8 and A11) and one horizontal plug (Figure A12).

The data fitting benefited very much from the composed model Dias/Cole-Cole, primarily for describing the intermediate frequency interval phase plateau, which has been associated to the various sample imperfections. We believe that also the non-convergence of the resistivity amplitudes for asymptotes at the lower and the higher frequencies, as for the samples of Figures A3, A4, A6, A9 and A11, can be also due to the mentioned sample imperfections.

It could be worthwhile to compare experimental data and its fitting curves for the pair of plugs coming from very close depths. In the case of the samples related to the curves A11 and A12 coming really from the same point, the first one a vertical plug and the second a horizontal, which permits to look at a true case of anisotropy.

Table 2 shows such analysis focusing on the diffusion effect (associated to the phase first maximum) and the capacitive effect (associated to the phase last maximum), and also on the amplitude main characteristics.

***Table 2** – Phase and amplitude comparative characteristics of the samples.*

Sample pair (plug orientation)	Depth spacing (cm)	Phase analysis		Amplitude analysis
		Diffusion effect	Capacitive effect	
A1(H), A2(H)	60	the same	A1 stronger	A2 more resistive > 2 times; both good convergence.
A5(H), A6(V)	30	A5 stronger	the same	A5 good convergence, more resistive > 3.5 times.
A7(H), A8(V)	60	A7 stronger	A8 stronger	both good convergence, A7 better. A8 more resistive 1.5 times.
A9(V), A10(H)	30	the same	A10 stronger	A10 good convergence, better, more resistive 3.5 times.
A11(V), A12(H)	0	A12 much stronger	A11 stronger	A12 good convergence, but not A11. A12 more resistive > 7 times.

It is interesting the fact that the horizontally oriented plugs exhibit a stronger diffusion effect. May appear that exists a tendency for a stronger capacitive effect be produced by the vertically oriented plugs.

Estimated hydraulic permeability from spectral electrical resistivity data

The estimated values of permeability have been done through the electrical measurements of the plugs from Corvina wells, with two models, the original Dias model and the composed Dias/Cole-Cole model, using the expression (4) discussed by Barreto and Dias (2014).

$$k = \frac{D/\eta^2}{2\upsilon^2 (F-1)^2 F \times 0.987 \times 10^{-15}} \qquad (4)$$

where k is the permeability (mD); $D = 1{,}3 \times 10^{-9}$ (m^2/s) is the diffusion coefficient for the íon Na^+ at 25ºC, according to Bockris and Reddy (1970); η is the electrochemical parameter that belongs to the Dias model; υ is the cementation factor and $F = \phi^{-\nu}$ is the formation factor (Archie, 1942).

The estimated values have been confronted with the experimental values, as shown in Figure 2.

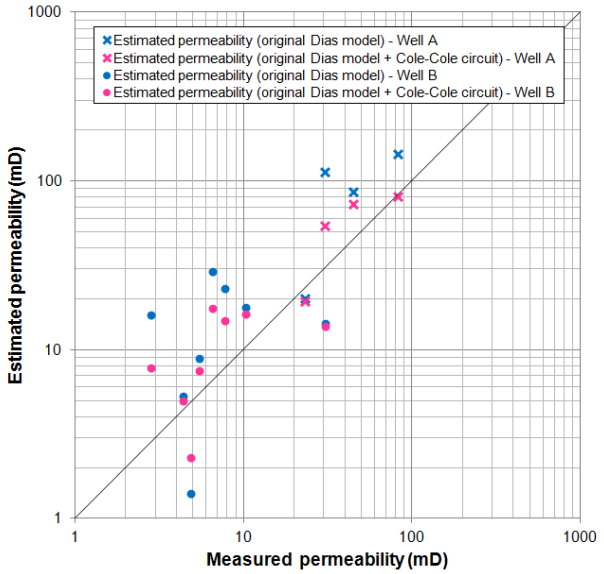

***Figure 2** – Correlation curve between the permeability experimental values represented on the horizontal axis and the estimated values, on the vertical axis, for samples from wells A (cross) and B (dots), blue colored (for the original Dias model) and in red (for the composed Dias/Cole-Cole model).*

Figure 2 shows that the two models produced very close values for the estimated permeability. That is because both models described almost equally well the first phase maximum. In general, a smaller error has been verified with the composed model (red colored values). Equally important is the direct relationship established by equation (4) between k and τ_w (phase first maximum relaxation time) through the parameter η. This permits to identify the

frequency interval where to look for determining k , as 10^{-3} Hz to 100Hz.

The logarithmic minimum-square error factors encountered for the estimated permeability values are: 2.70 for the original Dias model, 1.88 for the composed model, and 2.30 for all the values. The error factor function used (Tong *et. al*, 2006) is as follows:

$$[\ln(R)]^2 = \frac{1}{N}\sum_{j=1}^{N}[(\ln k_M(j) / k_E(j))]^2 \ , \qquad (5)$$

where k_M and k_E are, respectively, the measured and estimated permeability values and N is a number equal to 12 for each model and 24 for the two models together.

Conclusions

The complex resistivity measurements for the samples from the Corvina oil field wells and its modeling have been done successfully, using two models (the original Dias model and a new composed Dias/Cole-Cole model).

The samples in general presented strong imperfections like geometrical irregularities, presence of large and micro fractures, and, for the group B, incomplete saturation. We believe that such imperfections led to require a complimentary composed model for the data fitting.

The data fitting using the original Dias model produced significant discrepancies in an intermediate frequency interval, what has been solved by introducing the composed model. Both models, however, produced very close values for the permeability which are also good when compared to the measured values.

The frequency interval, where the electrical measurements should be done in order to afford the permeability, corresponds to the interval where the phase first maximum occurs, now determined as 10^{-3}Hz to 100Hz.

Acknowledgments

The authors thank LENEP/UENF for its excellent petrophysical laboratory infrastructure. We thank PETROBRAS for funding such infrastructure, and for financing this research. We also thank ANP/PETROBRAS for providing the samples of rock here analyzed.

References

Archie, G.E., 1942, The electrical resistivity log as an aid in determining some reservoir characteristics, Journal of Petroleum Technology, 1, 55-62.

Barreto, A. N. and Dias, C. A., 2014, Fluid salinity, clay content, and permeability of rocks determined through complex resistivity partition fraction decomposition. Geophysics, 79(5), D333-D347.

Bockris, J. O. and A. K. N. Reddy., 1970, Modern electrochemistry, Vols. 1, 2: Plenum Press.

Dias, C. A., 1968**,** A non-grounded method for measuring electrical induced polarization and conductivity: Ph.D. thesis, University of California–Berkeley.

Dias, C.A., 1972, An analytical model for a polarizable medium at radio and lower frequencies, J. Geophys. Res., 77, 4945-4956.

Dias, C. A., 2000, Developments in a model to describe low-frequency electrical polarization of rocks, Geophysics, 65, 2, 437-451.

Tong, M., Li, L., Wang, W., and Jiang, Y., 2006, A time domain induced-polarization method for estimating permeability in a shaly sand reservoir: Geophys. Prosp., 54, 623-631.

Worthington, A. E., Hedges, J. H., Pallat, N., 1990a, SCA guidelines for sample preparation and porosity measurement of electrical resistivity samples. Part I - Guidelines for preparation of brine and determination of brine resistivity for use in electrical resistivity measurements. The Log Analyst, 31, 20–28.

Worthington, P. F., Evans, R. J., Klein, J. D., Walls, J. D., White, G., 1990b, SCA guidelines for sample preparation and porosity measurement of electrical resistivity samples. Part III - the mechanics of electrical resistivity measurements on rock samples. *The Log Analyst*, 31, 2, 64–67.

Appendix A: Electrical data measured and modeled from Corvina wells

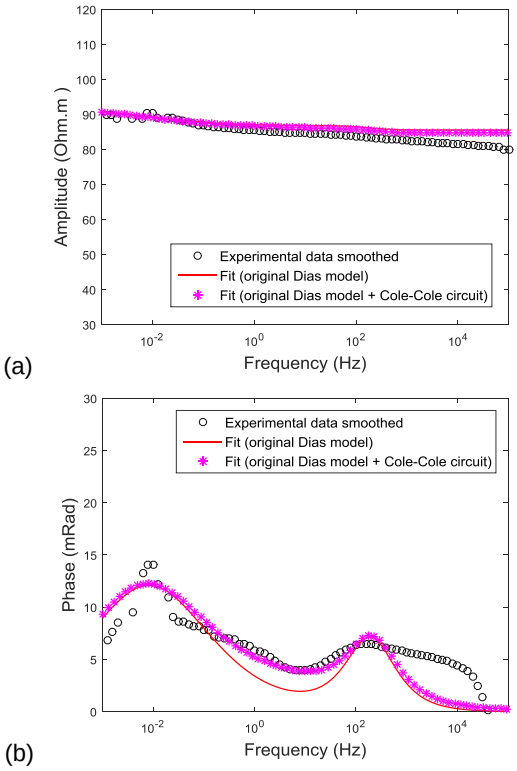

Figure A1 *- Experimental data and modeled curves from P0818H sample, well A: amplitude (a) and phase (b).*

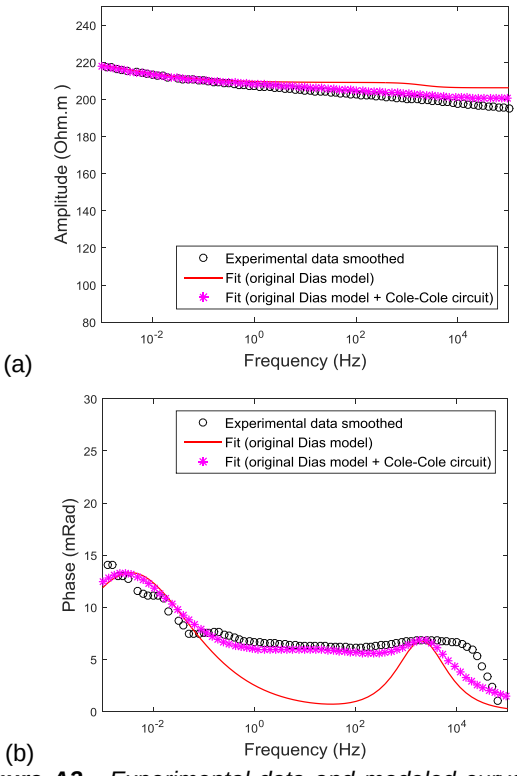

Figure A2 *- Experimental data and modeled curves from P0821H sample, well A: amplitude (a) and phase (b).*

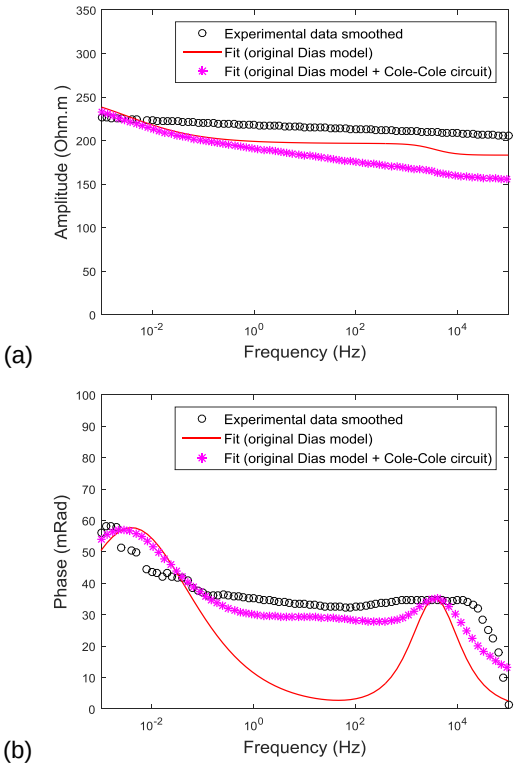

Figure A3 *- Experimental data and modeled curves from P0836H sample, well A: amplitude (a) and phase (b).*

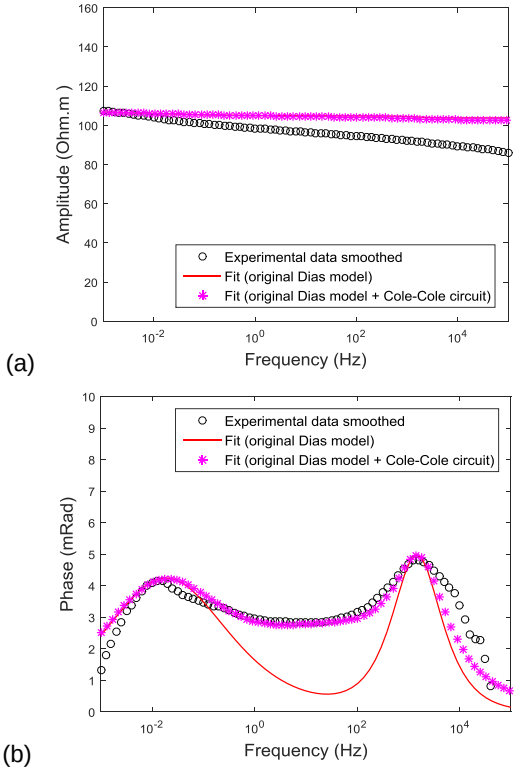

Figure A4 *- Experimental data and modeled curves from P0897H sample, well A: amplitude (a) and phase (b).*

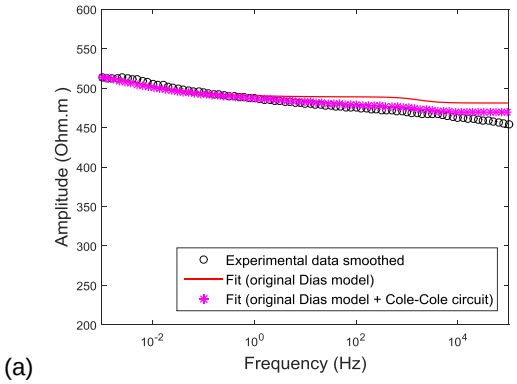

(a)

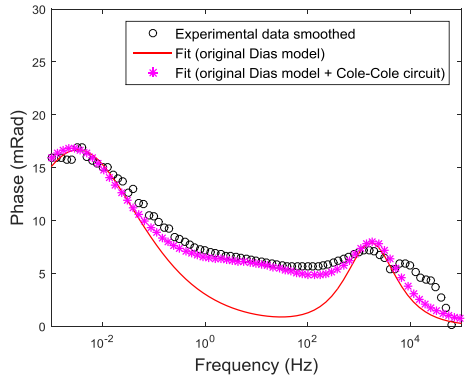

(b)

Figure A5 *- Experimental data and modeled curves from P3806H sample, well B: amplitude (a) and phase (b).*

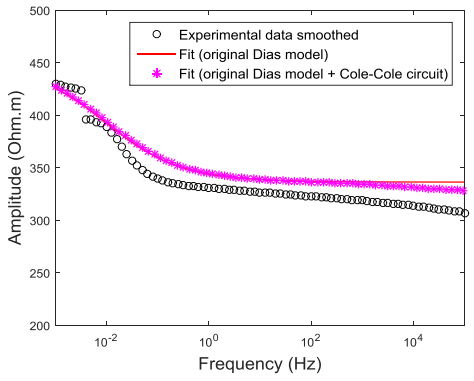

(a)

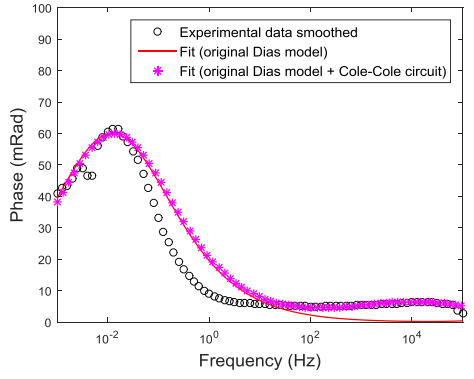

(b)

Figure A7 *- Experimental data and modeled curves from P3808H sample, well B: amplitude (a) and phase (b).*

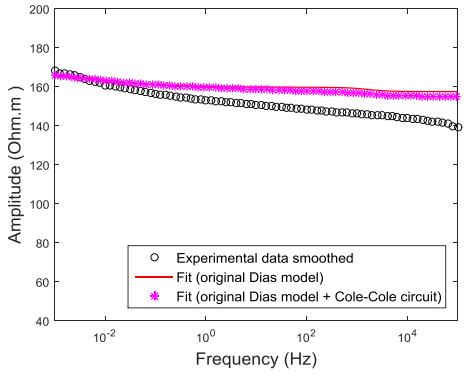

(a)

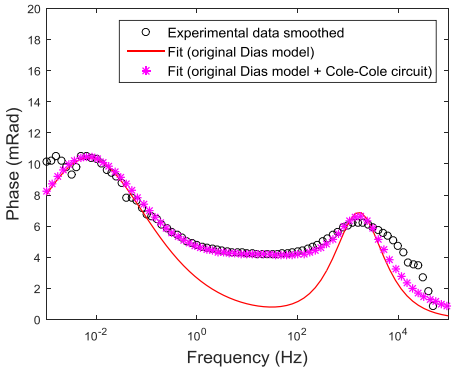

(b)

Figure A6 *- Experimental data and modeled curves from P3807V sample, well B: amplitude (a) and phase (b).*

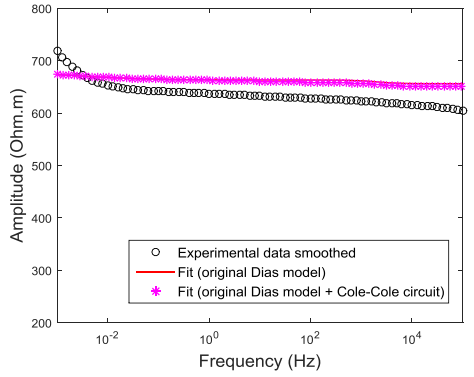

(a)

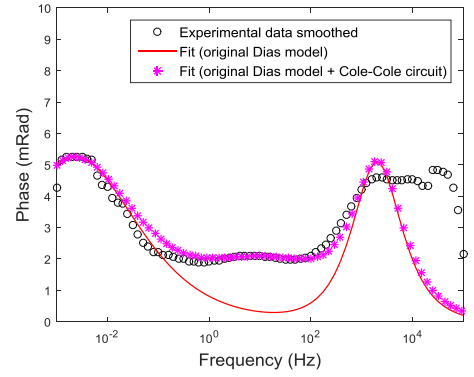

(b)

Figure A8 *- Experimental data and modeled curves from P3810V sample, well B: amplitude (a) and phase (b).*

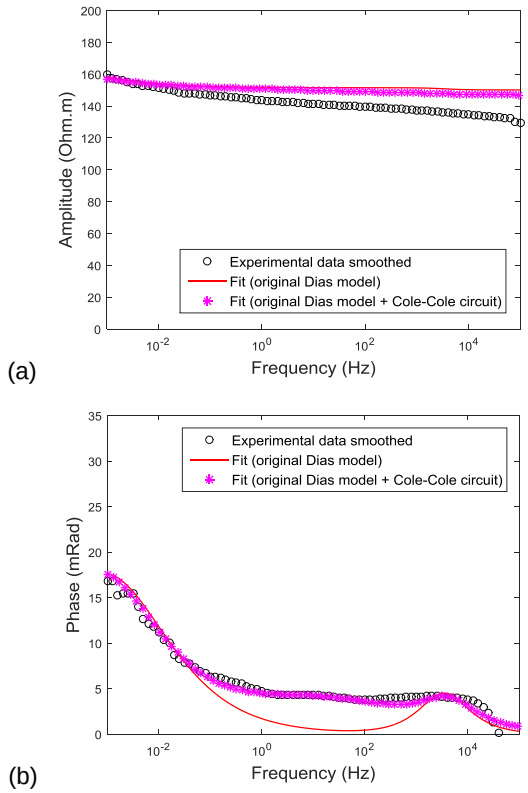

Figure A9 *- Experimental data and modeled curves from P3812V sample, well B: amplitude (a) and phase (b).*

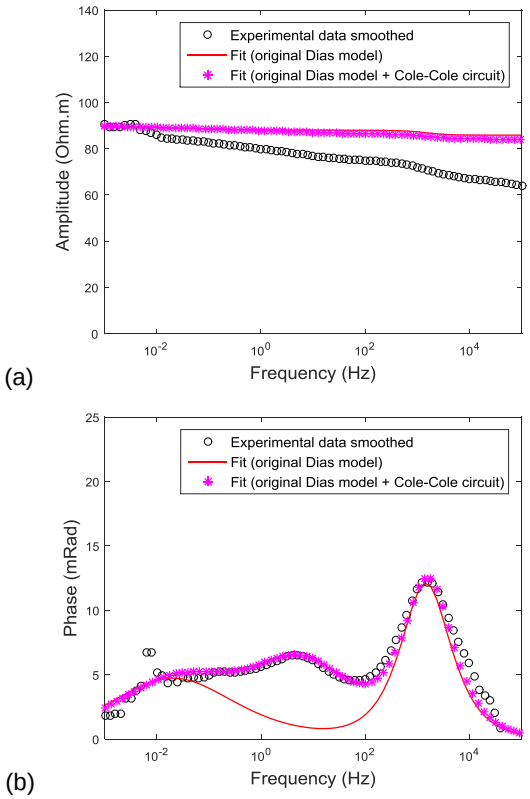

Figure A11 *- Experimental data and modeled curves from P3817V sample, well B: amplitude (a) and phase (b).*

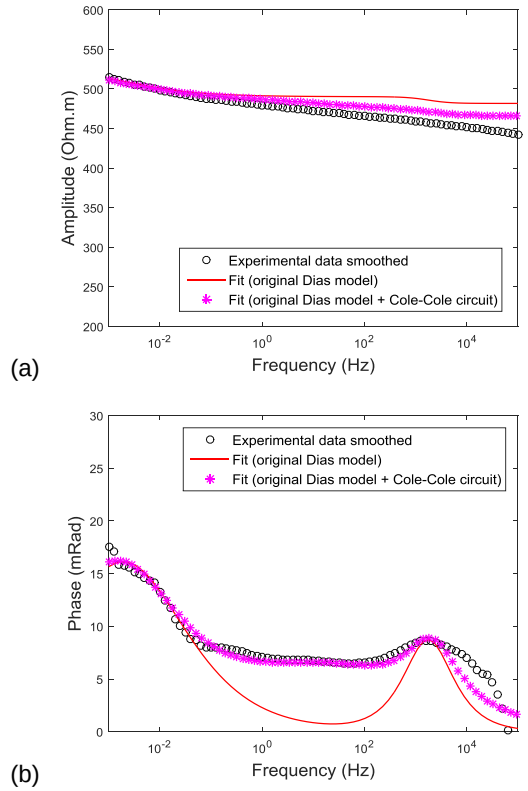

Figure A10 *- Experimental data and modeled curves from P3813H sample, well B: amplitude (a) and phase (b).*

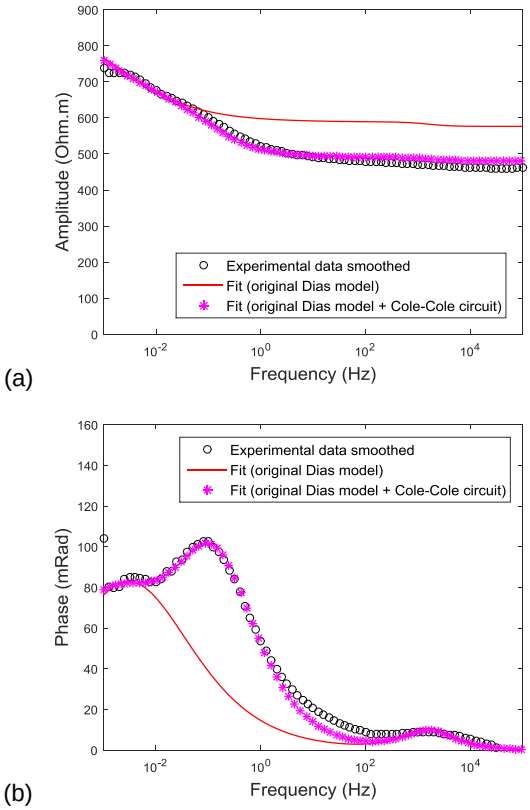

Figure A12 *- Experimental data and modeled curves from P3817H sample, well B: amplitude (a) and phase (b).*

Appendix B: Fitting parameters from "original Dias" and "original Dias + Cole-Cole Circuit" models

Table B1 *- Fitting parameters for well A samples.*

Sample P0818H	
Original Dias model	***Original Dias model + Cole-Cole circuit***
$\rho_0 = 92,0\Omega m$;	$\rho_0 = 92,0\Omega m$; $m = 0,080$;
$m = 0,070$; $\tau = 1,0\times10^{-3}s$;	$m_{w2} = 0,016$; $\tau = 9,0\times10^{-4}s$;
$\delta = 0,20$; $\eta = 1,17s^{-1/2}$	$\tau_{w2} = 6,4\times10^{-2}s$; $\delta = 0,18$;
	$\eta = 1,19s^{-1/2}$; c = 0,35
Approximate Dias model	***Approximate Dias model + Cole-Cole circuit***
$\rho_0 = 92,0\Omega m$;	$\rho_0 = 92,0\Omega m$; $m_{w1} = 0,060$;
$m_w = 0,057$; $m_D = 0,013$;	$m_{w2} = 0,016$; $m_D = 0,004$;
$\tau_w = 20,5s$; $\tau_D = 8,1\times10^{-4}s$;	$\tau_{w1} = 25,0s$; $\tau_{w2} = 6,4\times10^{-2}s$;
$f_a = 0,189$; $\nu = -1,4\times10^{-2}$	$\tau_D = 7,5\times10^{-4}s$; $f_a = 0,168$;
	$\nu = -1,3\times10^{-2}$; $c = 0,35$
Sample P0821H	
Original Dias model	***Original Dias model + Cole-Cole circuit***
$\rho_0 = 223\Omega m$;	$\rho_0 = 223\Omega m$; $m = 0,103$;
$m = 0,075$; $\tau = 9,5\times10^{-5}s$;	$m_{w2} = 0,039$; $\tau = 7,0\times10^{-5}s$;
$\delta = 0,18$; $\eta = 0,86s^{-1/2}$	$\tau_{w2} = 6,6\times10^{-3}s$; $\delta = 0,11$;
	$\eta = 1,15s^{-1/2}$; $c = 0,32$
Approximate Dias model	***Approximate Dias model + Cole-Cole circuit***
$\rho_0 = 223\Omega m$;	$\rho_0 = 223\Omega m$; $m_{w1} = 0,029$;
$m_w = 0,062$; $m_D = 0,013$;	$m_{w2} = 0,039$; $m_D = 0,035$;
$\tau_w = 47,5s$; $\tau_D = 7,9\times10^{-5}s$;	$\tau_{w1} = 75,9s$; $\tau_{w2} = 6,6\times10^{-3}s$;
$f_a = 0,169$; $\nu = -3,2\times10^{-3}$	$\tau_D = 6,3\times10^{-5}s$; $f_a = 0,100$;
	$\nu = -4,1\times10^{-3}$; $c = 0,32$
Sample P0836H	
Original Dias model	***Original Dias model + Cole-Cole circuit***
$\rho_0 = 260\Omega m$;	$\rho_0 = 260\Omega m$; $m = 0,420$;
$m = 0,295$; $\tau = 5,5\times10^{-5}s$;	$m_{w2} = 0,180$; $\tau = 4,0\times10^{-5}s$;
$\delta = 0,23$; $\eta = 0,79s^{-1/2}$	$\tau_{w2} = 8,8\times10^{-3}s$; $\delta = 0,14$;
	$\eta = 1,14s^{-1/2}$; $c = 0,25$
Approximate Dias model	***Approximate Dias model + Cole-Cole circuit***
$\rho_0 = 260\Omega m$;	$\rho_0 = 260\Omega m$; $m_{w1} = 0,050$;
$m_w = 0,244$; $m_D = 0,051$;	$m_{w2} = 0,190$; $m_D = 0,180$;
$\tau_w = 52,9s$; $\tau_D = 4,5\times10^{-5}s$;	$\tau_{w1} = 103,4s$; $\tau_{w2} = 8,8\times10^{-3}s$;
$f_a = 0,174$; $\nu = -2,2\times10^{-3}$	$\tau_D = 3,6\times10^{-5}s$; $f_a = 0,086$;
	$\nu = -3,1\times10^{-3}$; $c = 0,25$
Sample P0897H	
Original Dias model	***Original Dias model + Cole-Cole circuit***
$\rho_0 = 107\Omega m$;	$\rho_0 = 107\Omega m$; $m = 0,041$;
$m = 0,030$; $\tau = 1,6\times10^{-4}s$;	$m_{w2} = 0,017$; $\tau = 1,3\times10^{-4}s$;
$\delta = 0,33$; $\eta = 1,05s^{-1/2}$	$\tau_{w2} = 3,5\times10^{-3}s$; $\delta = 0,27$;
	$\eta = 1,14s^{-1/2}$; $c = 0,35$
Approximate Dias model	***Approximate Dias model + Cole-Cole circuit***
$\rho_0 = 107\Omega m$;	$\rho_0 = 107\Omega m$; $m_{w1} = 0,011$;
$m_w = 0,020$; $m_D = 0,010$;	$m_{w2} = 0,017$; $m_D = 0,013$;
$\tau_w = 8,7s$; $\tau_D = 1,1\times10^{-4}s$;	$\tau_{w1} = 11,2s$; $\tau_{w2} = 3,5\times10^{-3}s$;
$f_a = 0,323$; $\nu = -3,7\times10^{-3}$	$\tau_D = 9,6\times10^{-5}s$; $f_a = 0,262$;
	$\nu = -4,1\times10^{-3}$; $c = 0,35$

Table B2 *- Fitting parameters for well B samples.*

Sample P3806H	
Original Dias model	***Original Dias model + Cole-Cole circuit***
$\rho_0 = 530\Omega m$;	$\rho_0 = 530\Omega m$; $m = 0,115$;
$m = 0,092$; $\tau = 1,1\times10^{-4}s$;	$m_{w2} = 0,029$; $\tau = 9,0\times10^{-5}s$;
$\delta = 0,17$; $\eta = 0,88s^{-1/2}$	$\tau_{w2} = 17,7\times10^{-3}s$; $\delta = 0,14$;
	$\eta = 0,90s^{-1/2}$; $c = 0,39$
Approximate Dias model	***Approximate Dias model + Cole-Cole circuit***
$\rho_0 = 530\Omega m$;	$\rho_0 = 530\Omega m$; $m_{w1} = 0,085$;
$m_w = 0,078$; $m_D = 0,014$;	$m_{w2} = 0,029$; $m_D = 0,001$;
$\tau_w = 52,5s$; $\tau_D = 9,3\times10^{-5}s$;	$\tau_{w1} = 77,8s$; $\tau_{w2} = 17,7\times10^{-3}s$;
$f_a = 0,157$; $\nu = -3,6\times10^{-3}$	$\tau_D = 7,9\times10^{-5}s$; $f_a = 0,126$;
	$\nu = -3,5\times10^{-3}$; $c = 0,39$
Sample P3807V	
Original Dias model	***Original Dias model + Cole-Cole circuit***
$\rho_0 = 168\Omega m$;	$\rho_0 = 168\Omega m$; $m = 0,078$;
$m = 0,062$; $\tau = 1,2\times10^{-4}s$;	$m_{w2} = 0,023$; $\tau = 1,0\times10^{-4}s$;
$\delta = 0,22$; $\eta = 0,98s^{-1/2}$	$\tau_{w2} = 4,5\times10^{-3}s$; $\delta = 0,16$;
	$\eta = 1,26s^{-1/2}$; $c = 0,36$
Approximate Dias model	***Approximate Dias model + Cole-Cole circuit***
$\rho_0 = 168\Omega m$;	$\rho_0 = 168\Omega m$; $m_{w1} = 0,047$;
$m_w = 0,049$; $m_D = 0,013$;	$m_{w2} = 0,023$; $m_D = 0,008$;
$\tau_w = 23,8s$; $\tau_D = 9,5\times10^{-5}s$;	$\tau_{w1} = 28,2s$; $\tau_{w2} = 4,5\times10^{-3}s$;
$f_a = 0,209$; $\nu = -3,8\times10^{-3}$	$\tau_D = 8,5\times10^{-5}s$; $f_a = 0,149$;
	$\nu = -4,9\times10^{-3}$; $c = 0,36$
Sample P3808H	
Original Dias model	***Original Dias model + Cole-Cole circuit***
$\rho_0 = 450\Omega m$;	$\rho_0 = 450\Omega m$; $m = 0,330$;
$m = 0,305$; $\tau = 1,0\times10^{-8}s$;	$m_{w2} = 0,025$; $\tau = 1,0\times10^{-8}s$;
$\delta = 0,23$; $\eta = 1,40s^{-1/2}$	$\tau_{w2} = 1,4\times10^{-5}s$; $\delta = 0,24$;
	$\eta = 1,45s^{-1/2}$; $c = 0,45$
Approximate Dias model	***Approximate Dias model + Cole-Cole circuit***
$\rho_0 = 450\Omega m$;	$\rho_0 = 450\Omega m$; $m_{w1} = 0,190$;
$m_w = 0,253$; $m_D = 0,052$;	$m_{w2} = 0,025$; $m_D = 0,115$;
$\tau_w = 17,3s$; $\tau_D = 8,3\times10^{-9}s$;	$\tau_{w1} = 15,6s$; $\tau_{w2} = 1,4\times10^{-5}s$;
$f_a = 0,172$; $\nu = -5,3\times10^{-5}$	$\tau_D = 8,3\times10^{-9}s$; $f_a = 0,175$;
	$\nu = -5,4\times10^{-5}$; $c = 0,45$
Sample P3810V	
Original Dias model	***Original Dias model + Cole-Cole circuit***
$\rho_0 = 680\Omega m$;	$\rho_0 = 680\Omega m$; $m = 0,043$;
$m = 0,035$; $\tau = 1,1\times10^{-4}s$;	$m_{w2} = 0,010$; $\tau = 1,0\times10^{-4}s$;
$\delta = 0,29$; $\eta = 0,42s^{-1/2}$	$\tau_{w2} = 1,1\times10^{-2}s$; $\delta = 0,27$;
	$\eta = 0,44s^{-1/2}$; $c = 0,43$
Approximate Dias model	***Approximate Dias model + Cole-Cole circuit***
$\rho_0 = 680\Omega m$;	$\rho_0 = 680\Omega m$; $m_{w1} = 0,016$;
$m_w = 0,025$; $m_D = 0,010$;	$m_{w2} = 0,010$; $m_D = 0,017$;
$\tau_w = 70,9s$; $\tau_D = 7,9\times10^{-5}s$;	$\tau_{w1} = 75,6s$; $\tau_{w2} = 1,1\times10^{-2}s$;
$f_a = 0,283$; $\nu = -1,3\times10^{-3}$	$\tau_D = 7,4\times10^{-5}s$; $f_a = 0,261$;
	$\nu = -1,4\times10^{-3}$; $c = 0,43$

Sample P3812V	
Original Dias model + Cole-Cole circuit	***Original Dias model + Cole-Cole circuit***
$\rho_0 = 165\Omega m;$	$\rho_0 = 165\Omega m;$ $m = 0,110;$
$m = 0,090;$ $\tau = 5,0\times10^{-5}s;$	$m_{w2} = 0,020;$ $\tau = 4,0\times10^{-5}s;$
$\delta = 0,10;$ $\eta = 0,77s^{-1/2}$	$\tau_{w2} = 12,2\times10^{-3}s;$ $\delta = 0,06;$
	$\eta = 1,10s^{-1/2};$ $c = 0,34$
Approximate Dias model	***Approximate Dias model + Cole-Cole circuit***
$\rho_0 = 165\Omega m;$	$\rho_0 = 165\Omega m;$ $m_{w1} = 0,065;$
$m_w = 0,082;$ $m_D = 0,008;$	$m_{w2} = 0,025;$ $m_D = 0,020;$
$\tau_w = 200,0s;$ $\tau_D = 4,5\times10^{-5}s;$	$\tau_{w1} = 286,0s;$ $\tau_{w2} = 12,2\times10^{-3}s;$
$f_a = 0,092;$ $\nu = -2,4\times10^{-3}$	$\tau_D = 3,8\times10^{-5}s;$ $f_a = 0,054;$
	$\nu = -3,2\times10^{-3};$ $c = 0,34$
Sample P3813H	
Original Dias model + Cole-Cole circuit	***Original Dias model + Cole-Cole circuit***
$\rho_0 = 530\Omega m;$	$\rho_0 = 530\Omega m;$ $m = 0,124;$
$m = 0,091;$ $\tau = 1,1\times10^{-4}s;$	$m_{w2} = 0,044;$ $\tau = 8,5\times10^{-5}s;$
$\delta = 0,19;$ $\eta = 0,60s^{-1/2}$	$\tau_{w2} = 8,8\times10^{-3}s;$ $\delta = 0,13;$
	$\eta = 0,75s^{-1/2};$ $c = 0,31$
Approximate Dias model	***Approximate Dias model + Cole-Cole circuit***
$\rho_0 = 530\Omega m;$	$\rho_0 = 530\Omega m;$ $m_{w1} = 0,066;$
$m_w = 0,075;$ $m_D = 0,016;$	$m_{w2} = 0,044;$ $m_D = 0,014;$
$\tau_w = 89,9s;$ $\tau_D = 9,1\times10^{-5}s;$	$\tau_{w1} = 132,7s;$ $\tau_{w2} = 8,8\times10^{-3}s;$
$f_a = 0,176;$ $\nu = -2,4\times10^{-3}$	$\tau_D = 7,5\times10^{-5}s;$ $f_a = 0,116;$
	$\nu = -2,9\times10^{-3};$ $c = 0,31$
Sample P3817V	
Original Dias model + Cole-Cole circuit	***Original Dias model + Cole-Cole circuit***
$\rho_0 = 90,0\ \Omega m;$	$\rho_0 = 90,0\Omega m;$ $m = 0,065;$
$m = 0,046;$ $\tau = 2,2\times10^{-4}s;$	$m_{w2} = 0,021;$ $\tau = 2,0\times10^{-4}s;$
$\delta = 0,52;$ $\eta = 0,69s^{-1/2}$	$\tau_{w2} = 2,6\times10^{-2}s;$ $\delta = 0,53;$
	$\eta = 0,75s^{-1/2};$ $c = 0,60$
Approximate Dias model	***Approximate Dias model + Cole-Cole circuit***
$\rho_0 = 90,0\Omega m;$	$\rho_0 = 90,0\Omega m;$ $m_{w1} = 0,005;$
$m_w = 0,023;$ $m_D = 0,023;$	$m_{w2} = 0,021;$ $m_D = 0,039;$
$\tau_w = 8,1s;$ $\tau_D = 1,1\times10^{-4}s;$	$\tau_{w1} = 6,7s;$ $\tau_{w2} = 2,6\times10^{-2}s;$
$f_a = 0,508;$ $\nu = -1,8\times10^{-3}$	$\tau_D = 9,7\times10^{-5}s;$ $f_a = 0,513;$
	$\nu = -1,8\times10^{-3};$ $c = 0,60$
Sample P3817H	
Original Dias model + Cole-Cole circuit	***Original Dias model + Cole-Cole circuit***
$\rho_0 = 880\Omega m;$	$\rho_0 = 900\Omega m;$ $m = 0,465;$
$m = 0,345;$ $\tau = 1,0\times10^{-4}s;$	$m_{w2} = 0,157;$ $\tau = 1,0\times10^{-4}s;$
$\delta = 0,06;$ $\eta = 2,8s^{-1/2}$	$\tau_{w2} = 1,4s;$ $\delta = 0,06;$
	$\eta = 2,2s^{-1/2};$ $c = 0,71$
Approximate Dias model	***Approximate Dias model + Cole-Cole circuit***
$\rho_0 = 880\Omega m;$	$\rho_0 = 900\Omega m;$ $m_{w1} = 0,305;$
$m_w = 0,331;$ $m_D = 0,014;$	$m_{w2} = 0,157;$ $m_D = 0,003;$
$\tau_w = 79,2s;$ $\tau_D = 9,6\times10^{-5}s;$	$\tau_{w1} = 189,5s;$ $\tau_{w2} = 1,4s;$
$f_a = 0,040;$ $\nu = -1,3\times10^{-2}$	$\tau_D = 9,7\times10^{-5}s;$ $f_a = 0,033;$
	$\nu = -1,0\times10^{-2};$ $c = 0,71$